N O T I C E

THIS DOCUMENT HAS BEEN REPRODUCED FROM MICROFICHE. ALTHOUGH IT IS RECOGNIZED THAT CERTAIN PORTIONS ARE ILLEGIBLE, IT IS BEING RELEASED IN THE INTEREST OF MAKING AVAILABLE AS MUCH INFORMATION AS POSSIBLE

NASA Technical Memorandum 79286

COMPUTED VOLTAGE DISTRIBUTIONS AROUND SOLAR ELECTRIC PROPULSION SPACECRAFT

N. John Stevens
Lewis Research Center
Cleveland, Ohio

Prepared for the
Fourteenth International Conference on Electric Propulsion
sponsored by the American Institute of Aeronautics and Astronautics
and Deutsche Gesselschaft fur Luft- und Raumfahrt
Princeton, New Jersey, October 30-November 1, 1979

COMPUTED VOLTAGE DISTRIBUTIONS AROUND SOLAR ELECTRIC PROPULSION SPACECRAFT

by N. John Stevens
National Aeronautics and Space Administration
Lewis Research Center
Cleveland, Ohio 44135

INTRODUCTION

Space missions proposed for the future call for large, flexible systems launched by the Shuttle (refs. 1 to 4). These systems can either operate at Shuttle altitudes or be moved to geosynchronous orbits or beyond. One means of moving these large systems without exceeding their low acceleration requirements is by the use of electric propulsion thrusters (ref. 5). Electric propulsion is also proposed for scientific missions such as the comet explorers (refs. 6 and 7).

These spacecraft will require large, multikilowatt power sources for thruster operations. The conventional design of electric propulsion systems call for power to be generated at about 200 volts and use power processing to convert this into voltages required for thruster operations (ref. 8). However, a study for the proposed Halley Comet mission concluded that the net payload could be increased if a "direct drive" electric propulsion system is used (ref. 9). In this direct drive system, the high voltages required for thrusters ($\sim$1.2 kV) are generated directly on the solar array. Similar improvements in payload capability should also be realized for other direct drive electric propulsion missions.

It has been known since the early 70's that the geomagnetic substorm environment can charge spacecraft surface causing electronic switching anomalies and even satellite power system failures (e.g., see refs. 10 to 12). This spacecraft-charging phenomenon is under study in a joint AF/NASA investigation (ref. 13). The objective of this investigation is to develop techniques to control differential charging of geosynchronous satellites. Now, with the advent of much larger spacecraft that may have high-voltage surfaces exposed, these spacecraft-charging control techniques will be of greater importance to system designers. There have been several initial analytical treatments of large space system interactions with space environments (refs. 14 to 17) and preliminary treatments of electric thruster interactions with spacecraft and environments (refs. 18 and 19).

In this paper, the NASA Charging Analyzer Program (NASCAP) computer code (refs. 20 and 22) is used to compute voltage distributions around a Solar Electric Propulsion (SEP) spacecraft as it encounters an idealized geomagnetic substorm environment. Both a standard operating voltage and direct-drive voltage configuration are considered. The computations are presented first without thruster operations and then with a simplified, simulated thruster-on representation for direct-drive configuration only. It should be stressed that these computations looking for possible areas of concern in the spacecraft design are exploratory. Future improvements in

modelling resulting from such initial studies will enhance the value of computer codes as design tools.

ANALYTICAL MODEL

NASCAP Description

The NASA Charging Analyzer Program (NASCAP) has been described previously in the literature (refs. 20 and 22) and is only briefly summarized here. NASCAP is a quasistatic computational code, that is, it assumes that currents are functions of environmental parameters, electrostatic potential, and magnetostatic fields. It is capable of analyzing the charging of three-dimensional, complex bodies as a function of time for given space environmental conditions. It includes consideration of dielectric material properties (e.g., secondary emission, backscatter, photoemission, and bulk and surface conduction) and computes currents involving these materials in determining the surface voltages and potential distributions around the body.

In NASCAP, the body must be defined in terms of rectangular parallelipipeds, sections of parallelipides or flat plates within a 17x17x33 point grid. Seven separate conductors can be specified with the first conductor capable of floating with respect to space while the others can be biased with respect to the first. The environment can be defined in terms of single or double Maxwellian distributions (ref. 23) by specifying electron and proton temperatures (in electron volts) and plasma number densities. The code outputs a variety of graphic displays showing the model used, the voltage distributions for given environments at specified times, and particle trajectories (if desired).

The code can simulate low-density particle emitters either electrons or protons. Initial voltages, current density, and angles can be specified and the emission of either species computed for the field distribution around the body. If the charged particles escape, they are counted in the overall current balance and the potential of the floating conductor adjusted accordingly. The code can not yet treat particle-to-particle interactions. Hence, an accurate treatment of ion thruster fluxes is not possible.

Discharges on the surfaces of the body can also be simulated by NASCAP code. At a specified voltage difference between an insulator surface and the conductor beneath, a specified fraction of the charge deposited on the insulator will be transferred to the conductor beneath, the potential distributions readjusted for the charge redistribution, and the charging process continued. This simple discharge simulation is a representation of bulk breakdown through an insulator and can be used, in design studies, to pinpoint areas where large electrical stress can build up.

Spacecraft Description

The NASCAP model of the Solar Electric Propulsion spacecraft used in this report is shown in figure 1. It is representative of a 25-kilowatt version of such spacecraft. Each square in the NASCAP model is 10mx10m to allow the 30mx10m spacecraft to fit within the NASCAP grid point limitations.

The solar array wings are each 10mx12m. They are modelled as thin flat plates with 0.015 cm (6 mil) silica cover glass on the cells and a 0.010 cm

(4 mil) Kapton substrate. The aluminum squares on the arrays represents the exposed metallic interconnects. Since NASCAP can not simulate small gaps, these interconnects must be lumped together as shown. This lumped area represents 5% of the total solar cell area and is a reasonable approximation to proposed designs. Each wing is divided into three areas which are at specified voltages relative to the spacecraft body. For the standard configuration, the three areas are ±50 volts each (±150 volts total) and for the direct drive configuration the three areas are at +400 volts (+1200 volts total). These voltage configurations are shown in figure 2.

The spacecraft body is modelled in two parts: a simulated experiment deck and thruster system. The experiment deck is modelled as an octagon 4m across x 1m thick. It is covered by 0.010 cm (4 mil) Kapton blanket with a 2mx2m square of exposed metal (instrument platform). The thruster system consists of a 2mx3mx4m section covered by 0.020 cm (8 mil) optical solar reflectors (OSR), 0.020 cm (4 mil) Kapton and aluminum (to simulate thruster areas), and a housekeeping section, 2mx2mx1m, covered by 0.010 cm (4 mil) Kapton. The experiment deck is connected to the thruster system by a metallic boom; both are assumed to be at spacecraft ground potential. The solar arrays are connected to the spacecraft body by fairly large metallic booms which are also assumed to be at spacecraft ground potential.

In this model the criteria for occurrence of discharges is based on an edge voltage gradient breakdown concept (ref. 24) with the breakdown voltages determined from laboratory test data. For the Kapton surfaces breakdowns are assumed to occur when electric fields exceed 1.5×10^5 volts/cm, and for both the OSR and silica cover slides when the field exceeds 5×10^4 volts/cm (ref. 25). The charge lost in a discharge is assumed to be 50% of the charge stored on the insulator surface just prior to the discharge. This is based on a study that indicated that not all of the stored charge in large area samples is removed in a discharge (ref. 26).

Space Environment

For this study an assumed geomagentic substorm environment is used (fig. 3). This environment, utilizing single Maxwellian electron and proton temperatures, illustrates the transient nature of substorm environments and allows evaluation of spacecraft designs over a range of space conditions. The plasma densities chosen are large but reasonable. Since it has been shown that the charging rate is a strong function of the number density (ref. 27), then use of the values in this model should promote rapid charging of the surfaces and minimize computer time to expose the areas of concern.

Solar illumination is used in this study with the angle of incidence at 27^o to the solar array normal. This simulates January or July conditions in orbit and enhances possible sun-shade differential charging.

DISCUSSION OF RESULTS

Standard Configuration

The response of selected surfaces on the spacecraft model to the substorm environment is shown in figure 4. In figure 4(a) the response of sur-

faces on the experiment deck is shown. Since the sunlit Kapton surfaces on the deck generally follow the spacecraft ground potentials, they are not plotted. In figure 4(b) the response of surfaces on the thruster system section are shown. The response of the -150 volt section of the solar array is shown in figure 4(c). The response of the other sections of the array are similar to that of this section.

The data in these figures indicates that the spacecraft ground responds to the substorm by charging at a slower rate than the shaded insulators (e.g., see fig. 4(a)). This is to be expected since the capacitance of the spacecraft as a whole is much larger than that of isolated insulators. This does indicate the development of differential charging on spacecraft that was assumed to be the cause of spacecraft charging effects (ref. 28). Note that the silica cover slides on the solar array are positive with respect to the interconnects (see fig. 4(c)). This is due to the photoand secondary emission characteristics of the silica.

Major discharges start between 7 and 8 minutes after encounter with the substorm. This is shown by the strong negative peaks in the spacecraft ground potentials in all three figures (the solar array potential is fixed relative to spacecraft ground and remains at this set bias throughout the simulation). The negative peak results from the NASCAP discharge simulation which requires that charge be transferred to the conductor beneath. The conductor voltage is then recalculated based on this new charge content. This is not a perfect simulation of discharges since it is known that charge can be lost to space in the discharge process (ref. 26). However, it does provide a graphic display of arcing rates. It can easily be seen that major arcs occur every 6 minutes in the first phase of the substorm (T_e = 8 keV) and continues at a rate of once per 8 minutes in the second phase of the substorm (T_e = 6 keV). It should be noted that the silica cover glass on the solar array does not discharge: the negative peaks shown simply follows the spacecraft ground (fig. 4(c)).

The charging/discharging characteristics in both the spacecraft ground and insulator voltage traces appear to be very regular in the first phase of the substorm. However, in the second phase irregularities begin to appear (note the 30 to 33 min data of fig. 4(a)). These are due to breakdowns on only parts of the spacecraft. The voltage distributions around the spacecraft at times of 31, 32, and 33 minutes are shown in figure 5. These figures show an end view through the center of the spacecraft. These irregularities could be an effect due to the large size of the spacecraft since it did not appear in models of smaller satellites studied (ref. 27). It should be investigated further.

In the third phase of the substorm (T_e = 3 keV) all discharges stop and the spacecraft comes into equilibrium with a spacecraft ground potential of about -1200 volts relative to space. The insulator surfaces also stabilize at their respective values with the largest voltage difference being in the shaded Kapton at about 800 volts (fig. 4(a)). This substantiates that there is an electron temperature threshold in order for discharges to occur. This study and others (e.g., ref. 27) indicates that this threshold is at an electron temperature of about 5 keV. When the spacecraft moves into a quiescent environment, it rapidly, but not drastically, looses its charge.

Direct-Drive Configuration

Without Thruster Operation: In this part of the study the spacecraft is assumed to move through the substorm with high voltages in the solar array and thrusters off. This is done to establish the behavior for comparison with the standard configuration and with the simuilated thruster-on performance to be discussed in the next section.

The charging behavior of the spacecraft in this configuration is shown in figure 6. In figure 6(a) the response of the experiment deck is shown. The response of the thruster system section and shaded OSR's is shown in figure 6(b). In figure 6(c), the response of the silica solar cell covers, interconnects and Kapton substrate of one of the 1200-volt sections are shown.

The first observation is that spacecraft ground is driven about 800 volts more negative than in the standard configuration. This is believed to be due to the high positive voltages in the array. The silica cover glass behavior is also different: it is now negative with respect to the interconnects (figs. 4(c) and 6(c)).

Discharges occur here as they do with the standard configuration but the regularity patterns have changed. In the standard configuration, large numbers of surfaces discharged at the same time setting up a regular charge-discharge sequence. In the direct-drive configuration the discharges start at about 10 minutes after substorm encounter (about 2 min later than in the standard configuration). Thereafter, it appears that breakdowns occur piecemeal with a few surfaces discharging at each computational time step rather than massive numbers of surfaces discharging periodically. This indicates that, while the high voltages could cause more discharges, they could be less intense.

The voltage distributions around the spacecraft for 16, 17, and 18 minute time steps are shown in figure 7. The principal difference that occurs is in the voltage distributions around the solar array. It is apparent that the high voltages in the array sections causes concentrations whereas the standard configuration has fairly uniform fields at the solar arrays (compare figs. 5 and 7).

When the third phase of the substorm (T_e = 3 keV) is encountered, the arcing again stops. The potentials appear to stabilize with the spacecraft ground at about -1800 volts and the highest voltage on the solar array wing at about -600 volts (fig. 6(c)). The insulators come to equilibrium values as determined by substorm conditions and leakage currents. When the satellite moves out of the substorm, the surface voltages all quickly relax (without discharges) to their normal, lower values.

With Simulated Thruster Operations: As stated previously, the NASCAP code can not yet simulate ion thruster operations in a self-consistent manner. For this study the available proton and electron emitters are operated alternately for short periods of time to simulate the effects of plasma emission on spacecraft behavior. This simulation neglects particle-to-particle interactions. However, this method should give a reasonable approximation to the spacecraft behavior if the alternating emission times are short compared to the charging times of the spacecraft surfaces.

The following sequence is used in this study (see fig. 8). First, the spacecraft is allowed to charge negatively in the geomagnetic substorm for

10 cycles (570 sec). Then, while still in the first phase of the substorm (T_e = 8 keV), protons with a 1 mA beam current and an energy spread of 20 eV to 2 keV are emitted for 3 milliseconds. This is to evaluate possible effects of accelerated and charge exchange plasma particles (ref. 29) on a negatively biased spacecraft. Then, electrons are emitted at a fixed beam current of 10 mA and energy of 1 keV. These values were selected to guarantee that the electrons would leave the spacecraft and thus influence ground potentials. After 10 seconds, the electron emission is terminated and proton emission initiated for a total of 0.013 second. The electron emission is again started with the beam current rediced to 0.5 mA for the next 20 seconds. As the final phase of this simulation sequence, it was decided to evaluate the effects of constant accelerated electron emission only on spacecraft behavior. This is accomplished by allowing the electron emitter to operate at 0.5 mA beam current and 1 keV accelerating potential for the last 770 seconds.

The results of this simulation are shown in figures 9 to 12. The computations of surface voltages for substorm conditions done are similar to the previous results. So, the discussion of results begins with the initiation of proton emission at 570 seconds into the simulation. In figure 9 the short operations with the protons being emitted are shown with an expanded time scale so that the effects could be illustrated. When the spacecraft is negatively biased as it is just prior to emitter operations, proton emission first causes the ground potential to become less negative and then slowly became more negative. This is believed to be due to protons returning to spacecraft surfaces generating secondaries which escape. This changes the overall spacecraft current balance causing the shift in ground potential. The change in potential in turn changes the attractive potential for protons which modifies the current balance again causing the trend to more negative potential. It must be stressed that the overall system current balance is important and that this balance changes according to environment and emitter characteristics which influences the vehicle potential. Note that these effects are caused by relatively low currents - of the 1 mA of emitted protons only 50 to 80% return.

When electrons are emitted, the spacecraft ground potential rapidly rises towards zero. It is interesting to note that insulators (such as the shaded Kapton experiment deck surface) follow spacecraft ground potential changes as predicted from ground-based simulation studies (ref. 30). Eventually, the fixed beam current causes the spacecraft ground to go positive. At this point in time, electron emission is stopped and proton emission initiated to relax the spacecraft ground potential towards zero again. The electron source is again initiated for 20 seconds and the spacecraft potential remains close to zero volts. Finally, the proton only emission tends to drive the spacecraft slightly negative again.

The NASCAP simiulations illustrate the effects of particle emissions on voltage distributions around the spacecraft (see fig. 10). Initially, the substorm has charged the spacecraft negative and the usual strong voltage distributions exist (see fig. 7). The initial proton emission does not change these distributions significantly (see fig. 10(a)). When electrons are emitted, spacecraft ground potential starts towards zero volts and the voltage distributions are significantly altered (figs. 10(b) and (c)). A voltage barrier (which reaches -500 volts relative to the spacecraft) builds

up. Had the emitted electron energies been less than the barrier voltage, then emission would have been cut-off. This cut-off of low energy electron emission has been demonstrated in the ATS-5 active charge control experiments (ref. 31). Proton emission tends to collapse this voltage barrier while the electrons tend to build it up. By alternating particle emissions in rather short time periods, the voltage distributions tend to remain rather constant (see figs. 10(d), (e), and (f)). This behavior is in agreement with ATS-6 active charge control experiments in which a plasma neutralizer system was used to demonstrate that ground potentials could be controlled by emission of both ions and electrons (ref. 31).

It should be noted that there are still strong electric fields that can exist during particle emissions (fig. 10). These are at the high voltage areas of solar arrays, shaded areas on the experiment deck, and shaded areas on the thruster system section. Discharges did occur in these areas during this simulation. However, they are not the major discharges that occur simultaneously in a large number of cells and cause noticeable negative peaks in the spacecraft potential.

Proton particle trajectories are interesting to view and a selection of these trajectories that occurred after spacecraft potentials were controlled is shown in figure 11. Under these conditions, there is no measurable current returning to the spacecraft surfaces - it all escapes to space. One of the supositions made to explain the ATS-6 active charge control experiment results was that the ions returned to the spacecraft neutralizing the surface charge which allowed the electrons to escape controlling the spacecraft potential. Yet, in this case, the surfaces are negative but the protons do not return. It could be that the positive charges effectively reduce the barrier electric fields built up around the differentially charged spacecraft and this allows the electrons to escape. This is another topic for additional study.

Since it has been found that alternating electron and proton emission appears to exercise beneficial control over spacecraft behavior in a charging environment, then ion thrusters should be a practical means of providing this emission. Not only would they produce thrust but they could supply the relatively low currents of both electrons and ions required to control spacecraft potentials.

Finally, the evaluation of high energy electron only emission is shown in figures 12(a) and (b). In these figures the time scale starts at 470 seconds when the spacecraft is in the substorm and goes through the whole particle emission sequence. This discussion is limited to phase 7 simulation only. Electron emission with an accelerated beam does appear to control spacecraft ground potentials. However, it does not seem to influence the insulator potentials. The results indicate that differential voltages build up to a point where large areas discharge. This occurs on the solar array and the experiment deck.

CONCLUDING REMARKS

The NASCAP computer code has been used to conduct preliminary computations of the voltage distributions around large spacecraft in geomagnetic substorms. These spacecraft are possible configurations for future solar electric propulsion missions. Both a standard operating voltage configura-

tuion (±150 volt array) and a direct-drive configuration (+1200 volt array) are considered. The computations are made with the thruster-off for both configurations and with a thruster-on simulation (electrons and protons emitted) for the direct-drive configuration only.

As with other satellites in geosynchronous orbit, it has been found that geomagnetic substorms can charge these spacecraft surfaces to strong negative potentials. Arc discharges in the standard and direct-drive configurations without operating emitters are highly probable. It appears that discharges in the direct-drive configuration are more infrequent, but less intense.

It has been found that control of spacecraft voltages can be maintained by emission of relatively low currents; for example, 1 to 10 mA. It has also been found that alternating proton and electron emissions seems to control voltage destributions around the spacecraft and minimize the voltage barriers developed due to differential charging. This allows the spacecraft ground potentials to remain close to plasma potential. When the spacecraft ground is close to zero volts, protons all tend to escape. Since solar electric propulsion spacecraft have the inherent capability to emit both ions and electrons, they have a built-in active charge control technique.

When only high energy electrons are emitted, the spacecraft ground potential can be controlled. However, differential charging does cause the development of a 500-volt barrier at the emitter. The insulator surface voltages are not significantly affected by this type of emission and eventuallay large area discharges are observed.

This study is a preliminary one, looking principally at possible effects of the environment on large spacecraft. The simulation of ion thrusters used in this study is crude. It must be significantly improved to include simuiltaneous, interactive emission before more positive conclusions can be reached on the effects of ion thruster operations on spacecraft surfaces.

REFERENCES

1. "Outlook for Space", NASA SP-386, 1976.

2. Johnson, R.D. and Holbrow, C., eds., "Space Settlements, A Design Study," NASA SP-413, 1977.

3. Bekey, I., "Big COMSATS for Big Jobs at Low User Costs," Astronautics and Aeronautics, Vol. 17, Feb. 1979, pp. 42-56.

4. Savage, M. and Haughey, J, W., "Overview of Office of Space Transportation Systems Future Planning," Future Orbital Power Systems Technology Requirements, NASA CP-2058, 1978, pp. 71-92.

5. Woodcock, G. R., "Solar Satellites, Space Key to Our Future," Astronautics and Aeronautics, Vol. 15, July/Aug. 1977, pp. 30-43.

6. Dod, R. E., Austin, R. E., and Grim, D., "Solar Electric Propulsion for the Halley's Comet Rendezvous Mission - Foundation for Future Missions," AIAA Paper 78-83, Jan. 1978.

7. Atkins, K. L. and Auston, R. E., "The Ion Drive Program: Comet Rendezvous and SEPS Progress Report," AIAA Paper 79-2066, Oct. 1979.

8. Austin, R. E., "Solar Electric Propulsion Systems (SEPS): Tomorrow's Propulsion System Today," AIAA Paper 79-2045, Oct. 1979.

9. Poeschel, R. L., et al., "Extended Performance Solar Electric Propulsion Thrust System Study," Hughes Research Labs., Malibu, CA, Sep. 1977. (NASA CR-135-281, VOLS-1,2,4.)

10. Rosen, A., ed., Spacecraft Charging by Magnetospheric Plasmas, Progress in Astronautics and Aeronautics, Vol. 47, American Institute of Aeronautics and Astronautics, New York, 1976.

11. Pike, C. P. and Lovell, R. R., eds., Proceedings of the Spacecraft Charging Technology Conference, AFGL-TR-0051, NASA TM X-73537, Feb. 1977.

12. Spacecraft Charging Technology-1978, AFGL TR-79-0082, NASA CP-2071, 1979.

13. Lovell, R. R., Stevens, N. J., Schofer, W., Pike, C. P., and Lehn, W. L., "Spacecraft Charging Investigation: A Joint Research and Technology Program," Spacecraft Charging by Magnetospheric Plasmas, A. Rosen, ed., Progress in Aeronautics and Astronautics, Vol. 47, American Institute of Aeronautics and Astronautics, New York, 1976, pp. 3-14.

14. Purvis, C. K., Stevens, N. J., and Berkopec, F. D., "Interaction of Large, High Power Systems with Operational Orbit Charged Particle Environments," NASA TM-73867, 1977.

15. Stevens, N. J., "Space Environmental Interactions with Spacecraft Surfaces," NASA TM-79016, 1979.

16. Stevens, J. J. Roche, J. C., and Grier, N. T., "Large System-Charged Particle Environment Interaction Technology," NASA TM-79156, 1979.

17. Parker, L. W., "Plasma Sheath Effects and Voltage Distributions of Large High-Power Satellite Solar Arrays," Spacecraft Charging Technology-1978, AFGL TR-79-0082, NASA CP 2071, 1979, pp. 341-357

18. Parks, D. E. and Katz, I., "Spacecraft-Generated Plasma Interactions with High Voltage Solar Array," AIAA Paper 78-673, Apr. 1978.

19. Liemohn, H. B., Copeland, R. L., and Leavens, W. M., "Plasma Particle Trajectories Around Spacecraft Propelled by Ion Thrusters," Spacecraft Charging Technology-1978, AFGL TR-79-0082, NASA CP 2071, 1979, pp. 419-436.

20. Katz, I., Cassidy, J. J., Mandell, M. J., Schneulle, G. W., Steen, P. G., and Roche, J. C., "The Capabilities of the NASA Charging Analyzer Program," in Spacecraft Charging Technology-1978, AFGL TR 79-0082, NASA CP 2071, 1979, pp. 101-122.

21. Katz, I., Cassidy, J. J., Mandell, M. J., Schneulle, G. W., Steen, P. G., Parks, D. E., Rotenberg M., and Alexander, J. H., "Extension Validation and Application of the NASCAP Code," Systems Science and Software, La Jolla, CA, Jan. 1979. (NASA CR-159595.)

22. Cassidy, J. J., III. "NASCAP User's Manual-1978," Systems Science and Software, La Jolla, CA, Aug. 1978. (NASA CR-159417.)

23. Garrett, H. B., "Modelling of the Geosynchronous Plasma Environment," Spacecraft Charging Technology-1978, AFGL TR-79-0082, NASA CP-2071, 1979, pp. 11-22.

24. Stevens, N. J., Purvis, C. K., and Staskus, J. V., "Insulator Edge Voltage Gradient Effects in Spacecraft Charging Phenomena," IEEE Trans. Nucl. Sci., Vol. NS-25, Dec. 1978, pp. 1304-1312.

25. Stevens, N. J., Berkopek, F. D., Staskus, J. V. Blech, R. A., and Narcisco, S. J., "Testing of Typical Spacecraft Materials in a Simulated Substorm Environment," Proceedings of the Spacecraft Charging Technology Conference, C. P. Pike and R. R. Lovell, eds., AFGL TR-77-0051, NASA TM X-73537, 1977, pp. 431-457.

26. Aron, P. R. and Staskus, J. V., "Area Scaling Investigations of Charging Phenomenon," in Spacecraft Charging Technology-1978, AFGL TR-79-0082, NASA CP-2071, 1979, pp. 485-506.

27. Stevens, N. J. and Roche, J. C., "NASCAP Modelling of Environmental-Charging-Induced Discharges in Satellites," NASA TM-79247, 1979.

28. McPherson, D. A. and Schober, W., "Spacecraft Charging of High Altitudes: The SCATHA Satellite Program," Spacecraft Charging by Magnetospheric Plasmas, Progress in Astronautics and Aeronautics, Vol. 47, American Institute of Aeronautics and Astronautics, New York 1976, pp. 15-30.

29. Kamatso, G. K. and Sellen, J. M. Jr., "Beam Efflux Measurements for a 30-cm Mercury Ion Thruster," AIAA Paper 76-1052, Nov. 1976.

30. Purvis, C. K., Staskus, J. V. Roche, J. C. and Berkopek, F. D., "Charging Rates of Metal-Dielectric Structures," in Spacecraft Charging Technology-1978, AFGL TR-79-0082, NASA CP-2071, 1979, pp. 507-523.

31. Barttlett, R. O. and Purvis, C. K., "Summary of the Two Year NASA Program for Active Control of ATS-5/6 Environmental Charging," Spacecraft Charging Technology-1978, AFGL-TR-79-0082, NASA CP-2071, 1979, pp. 44-58.

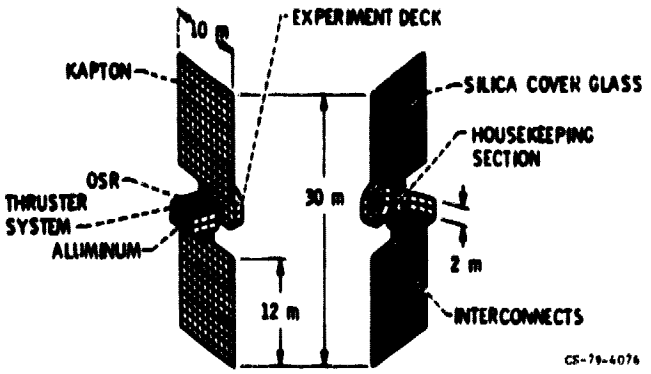

Figure 1. - NASCAP model solar electric propulsion spacecraft.

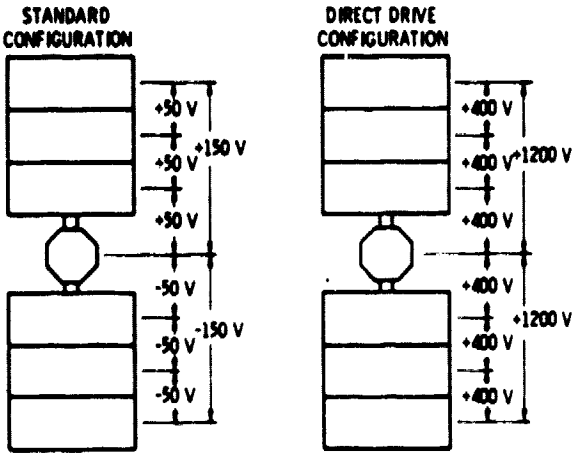

Figure 2. - Operating voltages on spacecraft configurations.

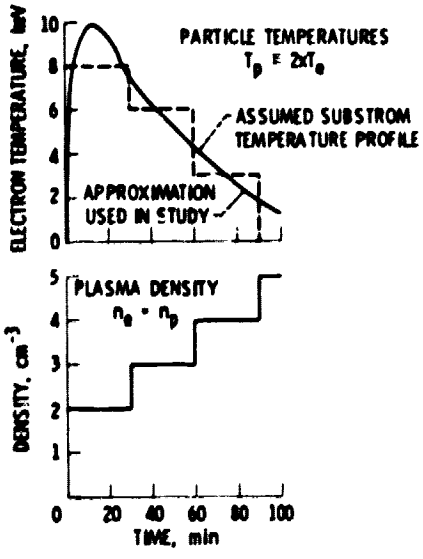

Figure 3. - Substorm environmental specification.

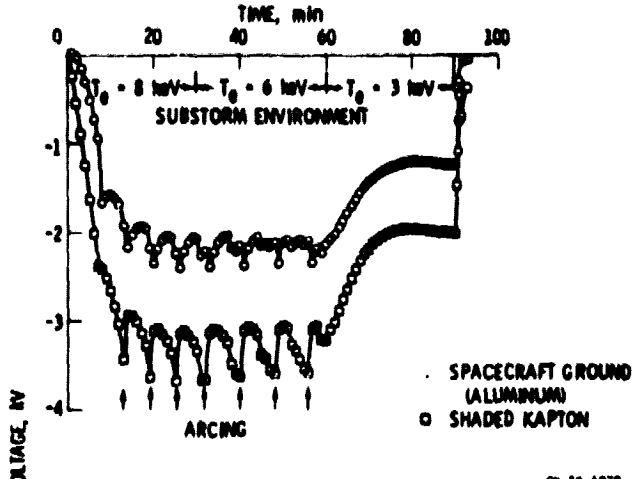

(a) EXPERIMENT DECK RESPONSE.

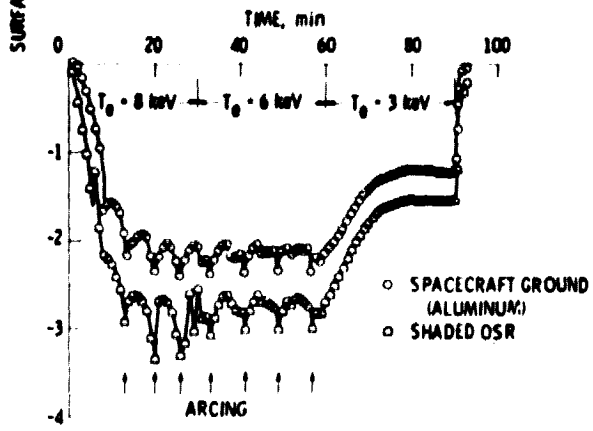

(b) THRUSTER SYSTEM RESPONSE.

Figure 4. - Standard configuration behavior.

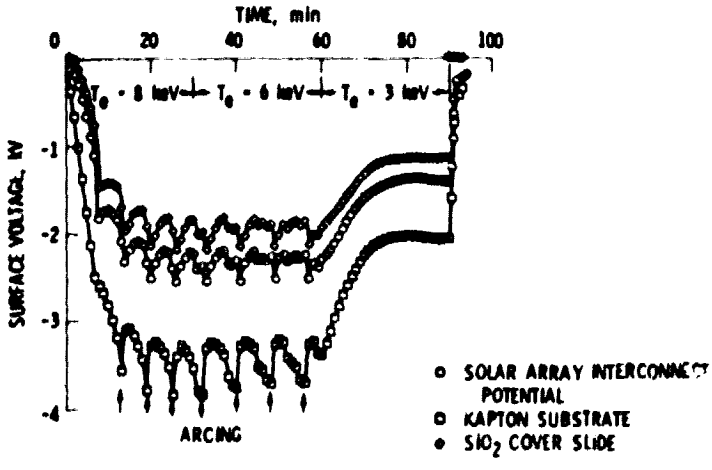

(c) TYPICAL SOLAR ARRAY RESPONSE.

Figure 4. - Concluded.

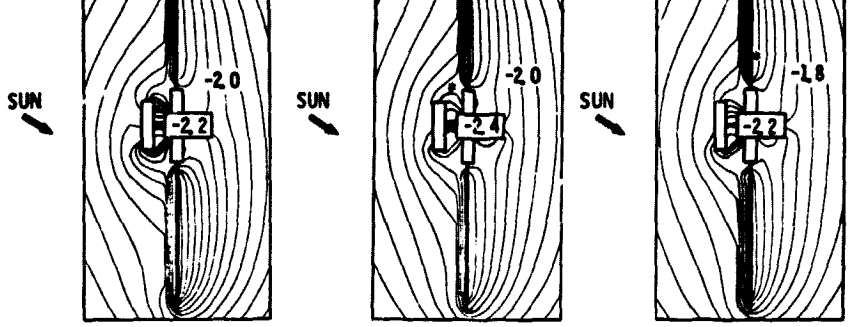

Figure 5. - Voltage distribution around spacecraft. Standard configuration; equipotential lines in 0.2 kV steps.

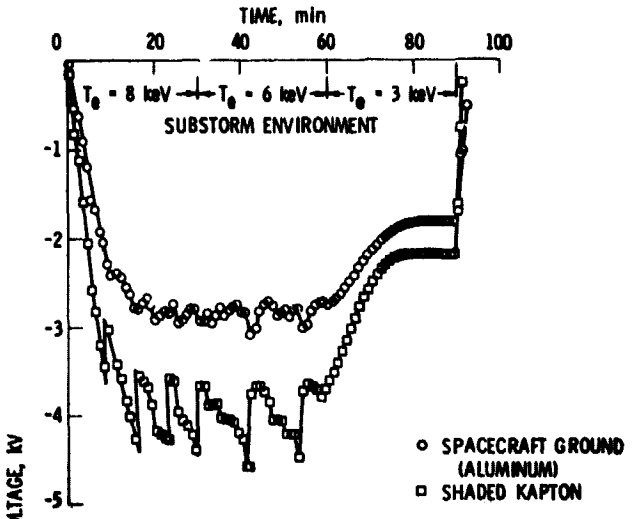

(a) EXPERIMENT DECK RESPONSE.

CS-79-4066

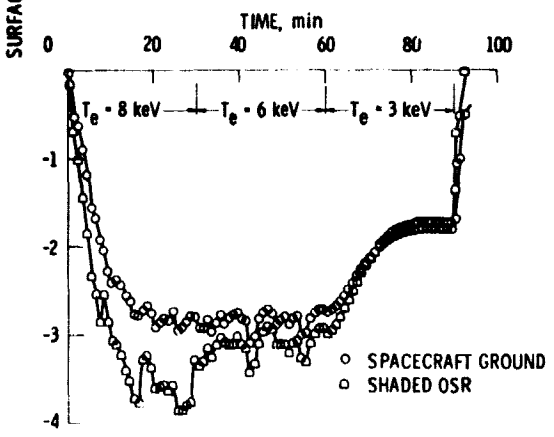

(b) THRUSTER SYSTEM RESPONSE.

Figure 6. - Direct drive configuration behavior.

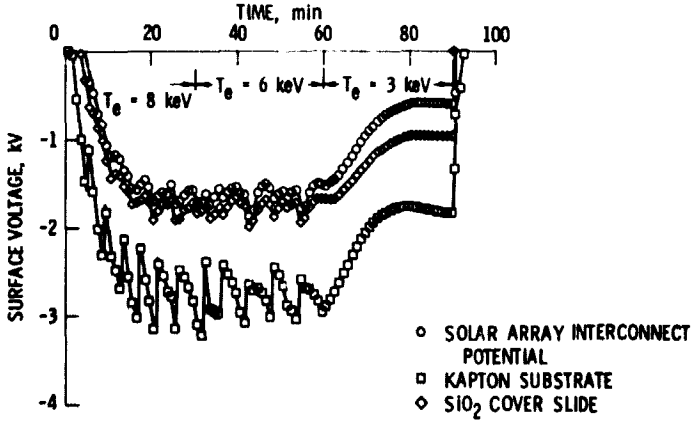

CS-79-4068

(c) TYPICAL SOLAR ARRAY RESPONSE; +1200 V SEGMENT.

Figure 6. - Concluded.

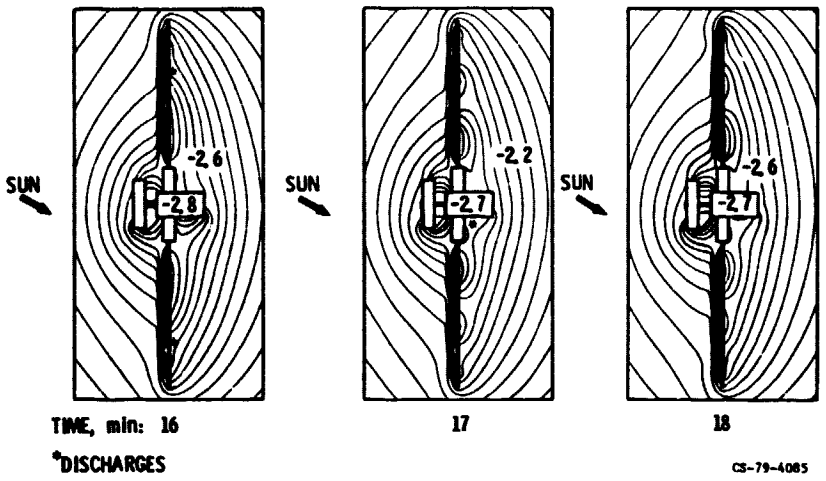

Figure 7. - Voltage distribution around spacecraft. Direct-drive configuration; equipotential lines in 0.2 kV steps.

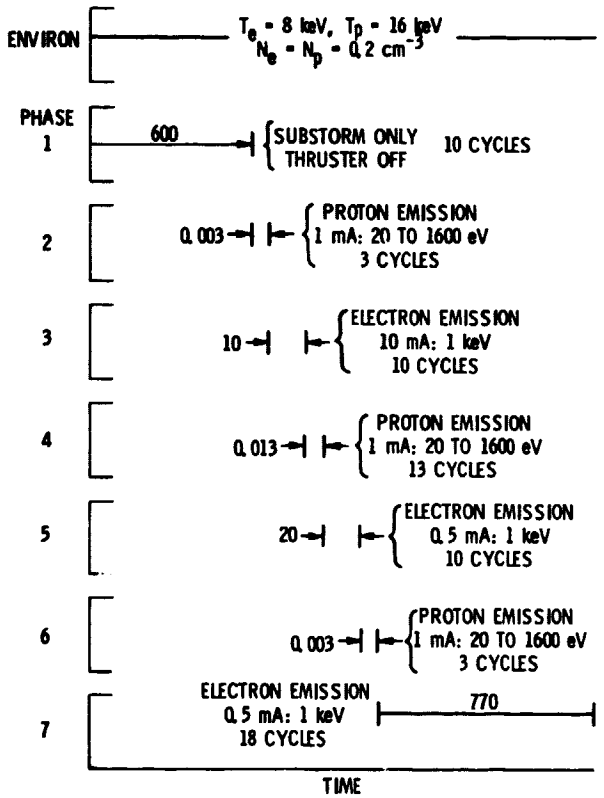

Figure 8. - Simulated thruster operational sequence.

CS-79-4083

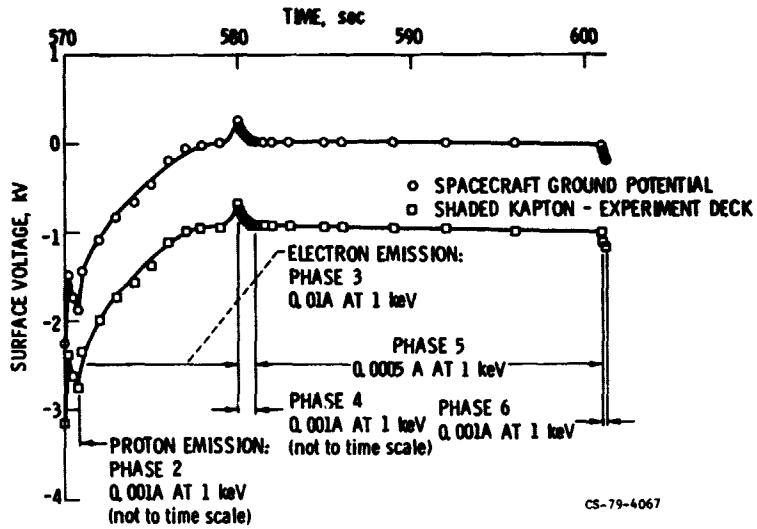

Figure 9. - Response of spacecraft during simulated thruster operation. Direct-drive configuration in substorm.

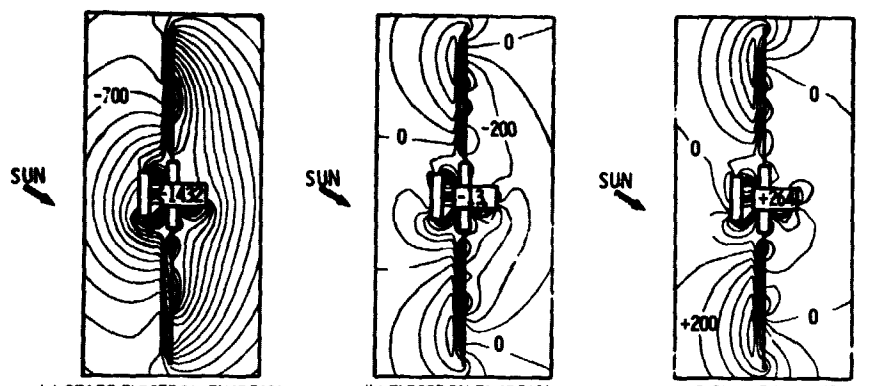

	(a) START ELECTRON EMISSION.	(b) ELECTRON EMISSION.	(c) END ELECTRON EMISSION.
PHASE:	3	3	3
CYCLE:	14	21	23
TIME, sec:	571	578	580

CS-79-4075

Figure 10. - Voltage distribution around spacecraft. Direct drive configuration in substorm: thruster simulation: equipotential lines in 100 V steps.

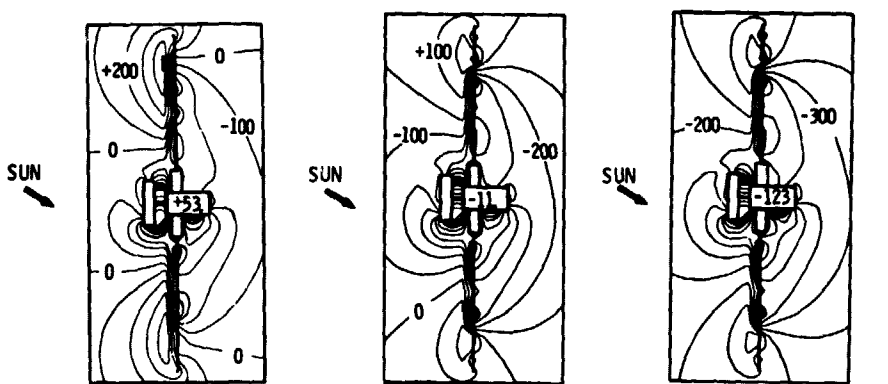

	(d) PROTON EMISSION.	(e) END ELECTRON EMISSION.	(f) PROTON EMISSION.
PHASE:	4	5	6
CYCLE:	34	46	48
TIME, sec:	580	600	601

CS-79-4074

Figure 10. - Concluded.

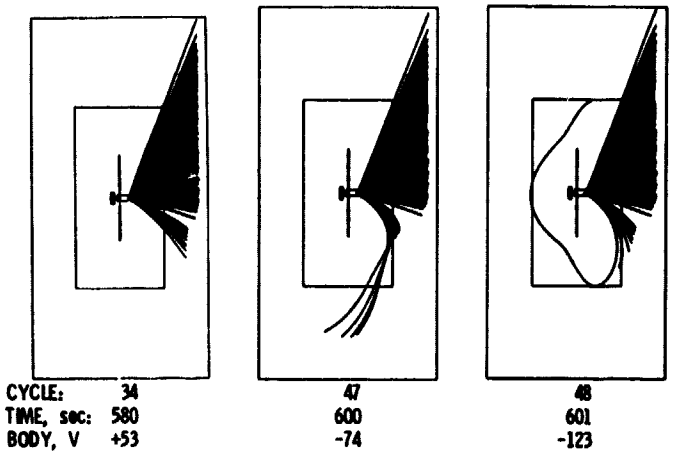

Figure 11. - Particle trajectories - protons. Beam current: 1 mA; energy range: 20 to 1500 eV; current returned to spacecraft: 0 A.

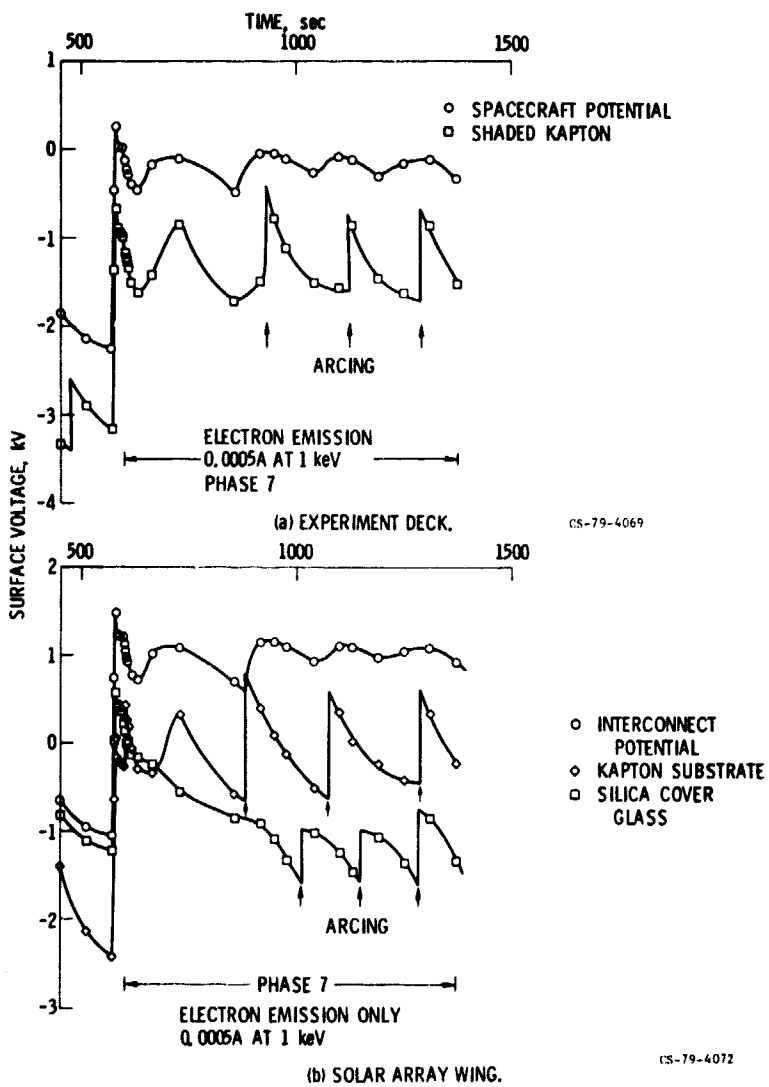

Figure 12. - Response to electron emission only. Direct-drive configuration in substorm.

1. Report No.	2. Government Accession No.	3. Recipient's Catalog No.
NASA TM-79286		

4. Title and Subtitle	5. Report Date
COMPUTED VOLTAGE DISTRIBUTIONS AROUND SOLAR ELECTRIC PROPULSION SPACECRAFT	6. Performing Organization Code
7. Author(s)	8. Performing Organization Report No.
N. John Stevens	E-225
	10. Work Unit No.
9. Performing Organization Name and Address	11. Contract or Grant No.
National Aeronautics and Space Administration Lewis Research Center Cleveland, Ohio 44135	13. Type of Report and Period Covered
12. Sponsoring Agency Name and Address	Technical Memorandum
National Aeronautics and Space Administration Washington, D.C. 20546	14. Sponsoring Agency Code

15. Supplementary Notes

16. Abstract

Solar electric propulsion spacecraft have been proposed for a variety of future missions. These spacecraft are characterized by large solar array wings and ion thrusters. In this study the NASA Charging Analyzer Program (NASCAP) is used to conduct preliminary computations of the voltage distributions around such large spacecraft in geomagnetic substorm environments at geosynchronous altitudes. Both a standard operating voltage (±150 volts on solar arrays) and direct-drive (+1200 volts on arrays) configurations are considered. Thruster-off simulations are computed for both operating voltage configurations while the effect of simulated thruster-on conditions are evaluated only for direct-drive configuration. These simulated thruster operations appear to alleviate surface charging.

17. Key Words (Suggested by Author(s))	18. Distribution Statement
Solar electric propulsion; Spacecraft interactions; Spacecraft charging; Geomagnetic substorm response; Electrostatic contamination	Unclassified - unlimited STAR Category 18

19. Security Classif. (of this report)	20. Security Classif. (of this page)	21. No. of Pages	22. Price*
Unclassified	Unclassified		

* For sale by the National Technical Information Service, Springfield Virginia 22161